# Magnetism and magnetic phase transition in nanowires of diamagnetically diluted superstrong magnets ε-$In_xFe_{1-x}O_3$

*A. I.* Dmitriev[1*] and M. S. Dmitrieva[1]

[1]Federal Research Center of Problems of Chemical Physics and Medicinal Chemistry RAS, Ac. Semenov avenue, 1, 142432 Chernogolovka, Russia

**Abstract.** The temperature dependences of magnetization of ordered arrays of diamagnetically diluted nanoparticles of superstrong ε-InxFe1-xO3 magnets (x = 0.04, 0.24) in cooling and heating mode in the permanent magnetic fields of different strengths - strong and weak compared to the magnetic anisotropy field - were measured. At temperatures of 150 K for x = 0.04 and 190 K for x = 0.24 a sharp drop in their magnetization is observed, practically to zero. Obtained evidence that the observed magnetic phase transition is accompanied by overturning of magnetization due to spin-reorientation transition of the first kind. The experimental results are described within the magnetodynamic and thermodynamic approaches.

## 1 Introduction

Iron (III) oxides exist in four basic polymorphic modifications: α-Fe2O3 (hematite), γ-Fe2O3 (magemite), ε-Fe2O3 and β-Fe2O3, each with different structural, electrical and magnetic properties [1-2]. Hematite is the most stable polymorph. Metastable ε-Fe2O3 has attracted attention in recent years because of its enormous coercive force value up to 20 kE at room temperature and its ability to absorb electromagnetic waves in the millimeter range [3-4]. All together this provides great potential for the applicability of ε-Fe2O3 for photocatalysis, gas sensors, magnetic/electrical tunable high-speed wireless communication devices and biomedical applications [5-10]. ε-Fe2O3 is not well suited for permanent magnet applications due to its low residual magnetization. It is expected to be used in high-density magnetic storage media requiring low residual magnetization, strong magnetic anisotropy and high coercive force so that thermal fluctuations do not lead to loss of magnetic moment orientation and loss of information [11-12].

Under conditions of strong anisotropy, the magnetic fields required to switch the magnetization direction (and hence to change the bit state of the memory cell) become unacceptably large. This marked the problem of developing a thermomagnetic way to record/erase information when the temperature of the magnetic medium crosses the compensation point or the spin reorientation temperature. Spontaneous spin reorientation

* Corresponding author: aid@icp.ac.ru

© The Authors, published by EDP Sciences. This is an open access article distributed under the terms of the Creative Commons Attribution License 4.0 (https://creativecommons.org/licenses/by/4.0/).

occurs in ε-Fe2O3 nanoparticles at T = 154 K [13]. The spin reorientation temperature in ε-Fe2O3 nanoparticles can be raised up to room temperature by diamagnetic dilution of ε-Fe2O3 by introducing various impurities In, Ga, Al [14-15]. From the above it can be concluded that studies of the magnetic phase transition parameters in ε-Fe2O3 are a priority for the field of modern materials science engaged in the search and creation of new materials for the element base of spintronics devices. The spin-reorientation transition in ε-Fe2O3 is accompanied by magnetic property anomalies. The dynamic magnetic susceptibility in the vicinity of the transition has a maximum [16], the coercive force passes through a minimum [17]. On this basis, ε-Fe2O3 nanoparticles near the spin-reorientation transition are attractive for use as magnetically soft and magnetostrictive materials.

The aim of the work is to establish the remagnetization mechanisms, to determine the microscopic parameters of the exchange interaction, to separate the high-temperature and low-temperature phase contributions to the total magnetization of nanoparticles, and to search for the magnetodynamic and thermodynamic regularities of the magnetic phase transition in them.

## 2 Methodology and materials of the experiment

ε-In0.04Fe1.96O3 nanoparticles (Fig. 1a) of spherical shape with an average diameter of 25 nm and ε-In0.24Fe1.76O3 (Fig. 1b) of nonspherical shape with length 80 nm and diameter 35 nm were fabricated by using two methods, inverse micelle synthesis and sol-gel method [14-15]. The nanoparticles were grown in a reverse micelle solution containing iron and indium nitrates. Nanoparticles were characterized by mass spectrometry, transmission electron microscopy, and X-ray diffraction [14-15]. The nanoparticles have an orthorhombic crystal structure with four non-equivalent cation positions of Fe3+ ions (Fig. 1c). However, one of them has a tetrahedral environment, and the other three have an octahedral environment. Indium ions are substitution impurities and are embedded in the octahedral positions of iron ions.

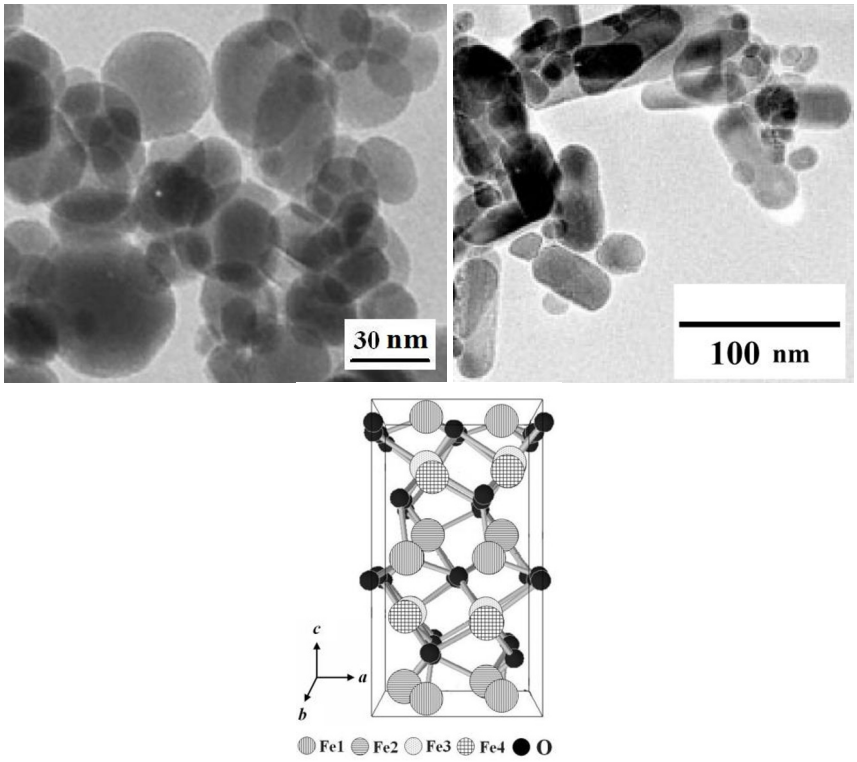


**Fig. 1.** Transmission electron microscope images of ε-In0.04Fe1.96O3 nanoparticles (a) and ε-In0.24Fe1.76O3 (b) as well as a schematic of their crystal structure (c)

The temperature dependences of the magnetic moment of nanoparticles were measured in the cooling and heating mode using a vibrating magnetometer of the multifunctional measuring cryomagnetic unit CFMS by Cryogenic Ltd, UK in various constant magnetic fields of strength H = 0.5 - 50 kOe in the temperature range

## 3 The results of experiments and discussion

### 3.1 ε-$In_{0.24}Fe_{1.76}O_3$ nanowires. Magnetodynamic approach

Figure 2 shows the temperature dependence of magnetization M(T) of ε-In0.24Fe1.76O3 nanowires in the magnetic field of 1 kOe, measured in the cooling mode.

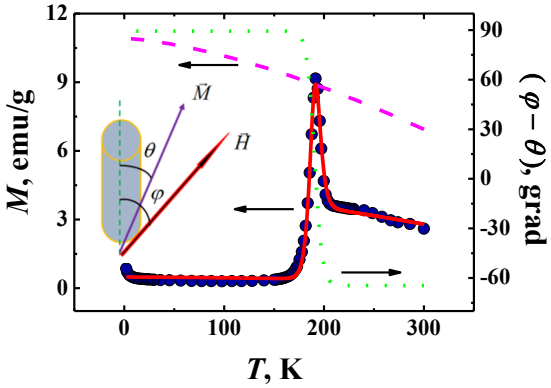


**Fig. 2.** Temperature dependence of magnetization M of ε-In0.24Fe1.76O3 nanowires measured in a magnetic field of strength 1 kOe in the cooling mode. The solid line shows the approximation. The dashed line shows the Bloch 3/2 dependence when □ - □ = 0. The dotted line shows the dependence of the angle difference □ - □. he inset shows the way the angles □ and □ *are counted*

At temperatures below TC = 414 K [14] the nanowires are in a magnetically ordered state as evidenced by the magnetic hysteresis loops on the dependence of M(H) with coercivity HC = 6 kOe at T = 300 K [18, 19]. At high temperatures T = 190 - 300 K an increase in magnetization with decreasing temperature is observed (Fig. 2). In the vicinity of 190 K there is a sharp decrease in magnetization to nearly zero, which remains almost constant with further decreases in temperature. Observed in the vicinity of 190 K magnetic phase transition, accompanied by a sharp decrease in magnetization, also leads to "collapse" of the hysteresis loop on the dependence of M(H), so that at a temperature of T = 100 K coercive force takes the value of HC = 200 Oe, ie dramatically decreases by 30 times [18, 19].

In the absence of an external magnetic field in a magnetically ordered crystal with magnetic anisotropy of the "light axis" type, the magnetization vector is directed along the light magnetization axis. Applying a magnetic field at some angle φ to the light axis causes the magnetization vector to rotate by an angle θ (see inset in Fig. 2). The magnetization of the sample measured in the magnetometer is the projection of the magnetization vector on the magnetic field direction:

$$M = M_S \cos(\phi - \theta), \tag{1}$$

where MS is the magnetization of saturation. In magnetically ordered crystals, the temperature dependence of magnetization is described by the Bloch 3/2 formula [5]:

$$M_S(T) = M_S(0)\left(1 - \mathrm{BT}^{3/2}\right), \tag{2}$$

where MS(0) is the magnetization of saturation at T = 0 K, B is the spin-wave parameter. The Bloch function 3/2 (2) increases with decreasing temperature, so the sharp decrease in magnetization to nearly zero in the vicinity of 190 K can be due to the multiplier containing a cosine in the expression (1). The angle θ is a function of the magnetic field and does not depend on temperature. Therefore, the only explanation for the sharp decrease in nanowire magnetization is a change in the angle φ, signifying the rotation of the light magnetization axis (spin-reorientation transition). To describe the dependence of φ(T), we chose a Heaviside-type step function:

$$\phi = \frac{\phi_0}{1+\exp(\mathrm{kT}-b)}. \quad (3)$$

*The solid line in Fig. 2 shows the approximation of the dependence M(T) by the system of equations (1-3). From the approximation, the parameters MS(0) = 11 emu/g, B = 7-10-5 K-3/2 were determined. In Fig. 2, the dashed dashed line shows the Bloch 3/2 dependence when* $\varphi$ - $\theta$ = 0. The dotted line shows the dependence of the angle difference $\varphi$ - $\theta$, где $\varphi(T)$, where φ(T) is described by expression (2) with parameters $\varphi_0$ = 154°, $k$ = 0.3 $K^{-1}$, $b$ = 51.

In the theory of spin waves, the parameter B included in the Bloch 3/2 formula (2) is related to the spin-wave stiffness coefficient D by the expression [20]:

$$B = 2.612\,\frac{g\mu_B}{M_S(0)}\left(\frac{k_B}{4\pi D}\right)^{3/2}, \quad (4)$$

where g = 2 is the g-factor of Fe3+ ions, S = 5/2 is the spin of Fe3+ ions, kB is the Boltzmann constant, μB is the Bohr magneton. The known values of B and MS(0) determined from the approximation of the dependence of M(T) (Fig. 2) allowed us to estimate the value of spin-wave stiffness D = 355 meV-Å2 (3-10-9 Oe-cm2). The values of spin-wave parameter B and spin-wave stiffness D are close to the corresponding values in similar materials: in γ-Fe2O3 nanoparticles B = 2.8-10-5 K-3/2, D = 440 meV-Å2 [21]; in Fe nanoparticles B = 4.8-10-5 K-3/2 [22], in Fe3O4 nanoparticles B = 3.5-10-5 K-3/2, D = 320 meV-Å2 [23].

The spin-wave stiffness coefficient D is related to the exchange integral J by the expression [24]:

$$J = \frac{\mathrm{D}g\mu_B}{2\mathrm{Sr}_S^2}, \quad (5)$$

where rs is the average distance between Fe3+ ions. Evaluation of the exchange integral by formula (5) gives the value J = 9.7 cm-1. On the other hand, the exchange integral can be estimated in the Weiss molecular field approximation by equating the average energy of the exchange interaction with the energy of thermal fluctuations [20]:

$$k_B T_C = \frac{2\mathrm{zJS}(S+1)}{3}, \quad (6)$$

where z = 6 is the number of nearest neighbors, TC = 414 K is the magnetic ordering temperature [14]. The value of the exchange integral $J$ = 8.2 $cm^{-1}$ calculated by formula (6) turned out to be close to the value determined by formula (5) and close to the theoretical estimates $J$ = 3.9 – 5.4 $cm^{-1}$ obtained in [14].

### 3.2 ε-$In_{0.04}Fe_{1.96}O_3$ nanowires. Thermodynamic approach

Fig. 3 shows the temperature dependences of magnetization of ε-In0.04Fe1.96O3 nanoparticles measured in the cooling and heating mode. When the temperature decreases, the magnetization growth is observed, which is replaced by a sharp decrease at the temperature TSR = 150 K. In the relatively narrow temperature range T = 75 to 150 K, the magnetization of the sample decreases almost to zero (Fig. 3). As the temperature increases, the sample adopts the initial magnetization value at higher temperatures, i.e., temperature hysteresis is observed. Hysteresis phenomena accompanying the formation of nuclei of another phase and the course of phase transformations with a finite rate are characteristic of phase transitions of the first kind. The temperature range T = 75 - 125 K, where temperature hysteresis is observed, corresponds to the region of coexistence of metastable

states. Domain walls usually serve as the germs of the new phase, since they always contain areas in which the direction of magnetization coincides with that in the new phase.

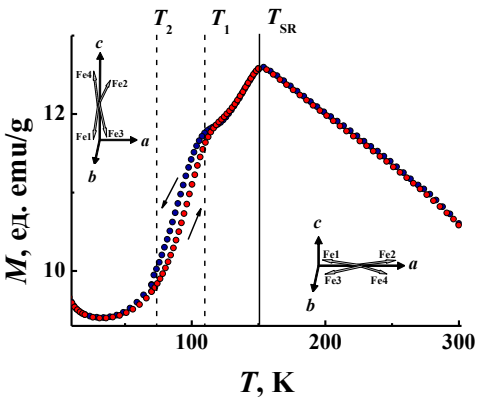


**Fig. 3.** Temperature dependences of magnetization of ε-In0.04Fe1.96O3 nanoparticles measured during cooling (blue symbols) and heating (red symbols). The solid vertical line indicates the spin-reorientation transition temperature TSR = 150 K. Dotted vertical lines indicate temperatures T1 and T2, corresponding to the metastable state of coexistence of both phases. The arrows indicate the directions of temperature change. The insets schematically show the directions of magnetization of each of the iron sublattices relative to the crystallographic axes in each of the phases

At present, the observed magnetic phase transition from a high-temperature phase (HTP) with a high magnetization value to a low-temperature phase (LTP) with a low magnetization value has been described using different approaches and approximations [11, 13, 17]. The key one among them is the magnetodynamic approach discussed above, according to which the observed magnetic phase transition is a spin-reorientation transition. This transition is characterized by the fact that, when the temperature changes, the orientation of magnetization with respect to the crystallographic axes (the axes of light magnetization) changes. In the general case, there are three possible phases. Two collinear phases with $\theta = 0, \pi$, $K1 \geq 0$ (BTF) and $\theta = \pi/2, 3\pi/2$, $K1 + 2K2 \leq 0$ (LTP) with light axis and light plane type anisotropy, respectively [25]. And the angular phase with $\sin 2\theta = -K1/2K2$, $K1 < 0$ and $K1 + 2K2 \geq 0$ c anisotropies of the light axis magnetization cone type [25]. Here $\theta$ is the angle specifying the orientation of the magnetization vector in the crystal, K1 and K2 are the first and second magnetic anisotropy constants. If K1 changes sign and $K2 > 0$ as the temperature changes, both collinear and angular phases can exist in the crystal. Spin reorientation occurs as two phase transitions of the second kind. When $K2 < 0$, the angular phase is unstable, and the temperature regions of existence of the collinear phases overlap (Fig. 4).

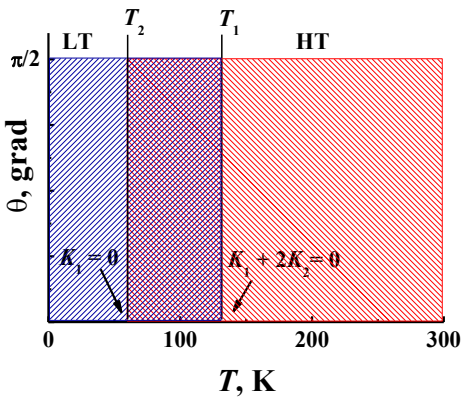


**Fig. 4.** Schematic of the phase diagram of ε-In0.04Fe1.96O3 nanoparticles in coordinates (θ, T). The areas with sloping shading correspond to each of the phases (LT and HT). The vertical lines indicate the temperatures T1 and T2, corresponding to the metastable coexistence state of both phases. The cross-hatching corresponds to this region. The overlapping boundaries of the regions of phase coexistence at temperatures T1 and T2 are given by the expressions K1(T2) = 0 and K1(T1) + 2K2 = 0 (see boxes)

Spin reorientation occurs as a single phase transition of the first kind. The change in the sign of the anisotropy constants of ε-Fe2O3 with temperature change is attributed to the competition of the single-ion and dipole-dipole anisotropy contributions, which have a different temperature dependence [13].

Another fundamental approach is the thermodynamic approach, which will be discussed below. For this purpose, we will use the model of Slichter and Drickamer [26], usually used to describe the thermodynamics of the transition from the low-spin to the high-spin state of transition metal ions at spin-crossing. In Slichter and Drickamer's work, the Gibbs energy is written in the form [26]:

$$G = (1-\gamma)G \quad + \gamma G_{HT} - TS_{mix} + g_{\int} \quad .$$

Here $G_{LT}$ *and* $G_{HT}$ – are the Gibbs potentials of HTP and LTP, respectively; γ is the reduced quantity of HTP; T is temperature; $S_{mix} = -k_B[\gamma\ln\gamma+(1-\gamma)\ln(1-\gamma)]$ is configuration entropy ($k_B$ is Boltzmann constant); $g_{int} = \Gamma\gamma(1-\gamma)$ is interaction energy (G is interaction parameter). The equation of phase equilibrium is obtained by equating the Gibbs energy derivative over the parameter γ to zero:

$$\frac{dG}{d\gamma} = -G \quad + G_{HT} + \Gamma(1-2\gamma) - k_B T ln\left(\frac{1-\gamma}{\gamma}\right) = 0 \qquad (7)$$

or

$$\Delta H - T\Delta S + \Gamma(1-2\gamma) - k_B T ln\left(\frac{1-\gamma}{\gamma}\right) = 0, \qquad (8)$$

where ΔH and ΔS are enthalpy and entropy changes during the magnetic phase transition. Solving equation (8), assuming that G → 0, we can write an equation describing the dependence of γ(T):

$$\gamma = \frac{1}{1+exp\left[\Delta H\left(\left(\frac{1}{T}-\frac{1}{T_{1/2}}\right)\right)\right]}, \qquad (9)$$

where $T_{1/2} = \Delta H/\Delta S$ temperature at which γ = 0.5 (equilibrium between HTP and LTP).

The temperature dependence of magnetization M(T) is determined by the contributions of the HTP and LTP magnetizations:

$$M(T) = (1-\gamma)M \quad + \gamma M_{HT}, \tag{10}$$

where $M_{LT}$ *and* $M_{HT}$ – magnetizations of HTP and LTP, respectively. The $M_{LT}$ *and* $M_{HT}$ values in the narrow temperature range of the magnetic phase transition can be assumed constant.

Fig. 5 shows fragments of the temperature dependences of the magnetization of ε-In0.04Fe1.96O3 nanoparticles in the vicinity of the temperature hysteresis, measured in different magnetic fields.

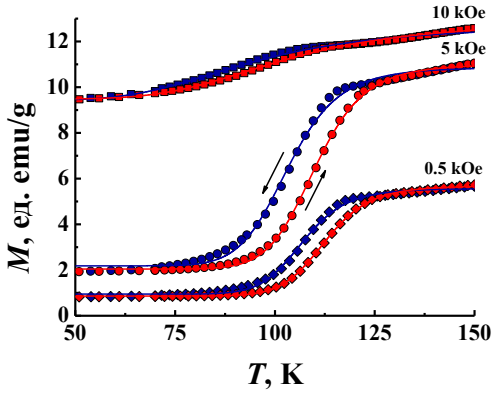


**Fig. 5.** Fig. 5 shows fragments of the temperature dependences of the magnetization of ε-In0.04Fe1.96O3 nanoparticles in the vicinity of the temperature hysteresis, measured in different magnetic fields.

The solid lines in Fig. 5 show the approximation using expression (10). From the approximation, the values of $M_{LT}$ *and* $M_{HT}$, magnetizations, enthalpy and entropy, as well as other thermodynamic characteristics of the discussed spin-reorientation transition registered in different magnetic fields were determined (Table 1).

**Table 1.** Thermodynamic characteristics of spin-reorientation phase transition in ε-In0.04Fe1.96O3 nanoparticles

| | $T_{1/2\downarrow}$, K | $T_{1/2\uparrow}$, K | $\Delta T$, K | $\Delta H$, kJ/mol |
|---|---|---|---|---|
| 0.5 kOe | 107.1 | 112.7 | 5.6 | 4.1 |
| 5 kOe | 103.4 | 110.2 | 6.8 | 13.9 |
| 10 kOe | 95.1 | 103.5 | 8.4 | 17.5 |

Fig. 6 shows an example of the temperature dependence of γ established from the approximation.

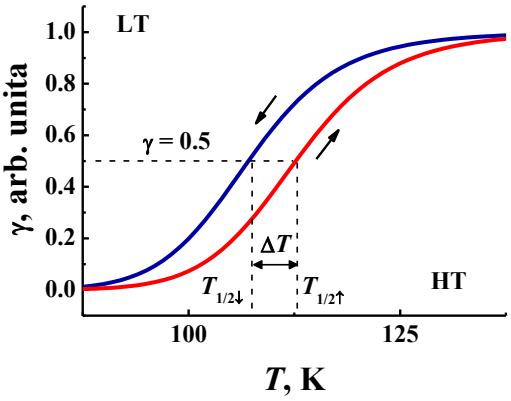


**Fig. 6.** Phase diagram of ε-In0.04Fe1.96O3 nanoparticles in coordinates (γ, T). The arrows indicate the directions of temperature change. The vertical dashed lines indicate the temperatures $T_{1/2\downarrow}$ and $T_{1/2\uparrow}$, at which γ = 0.5 (marked by the horizontal dashed line) corresponds to the LT and HT equilibrium. The difference $T_{1/2\uparrow} - T_{1/2\downarrow}$ *is the width of the spin reorientation temperature hysteresis* $\Delta T$

It follows from Table 1 that under the influence of the magnetic field of strength H there is a linear shift of reorientation temperatures ΔT(H) ~ H (Fig. 7), in agreement with theoretical notions [25].

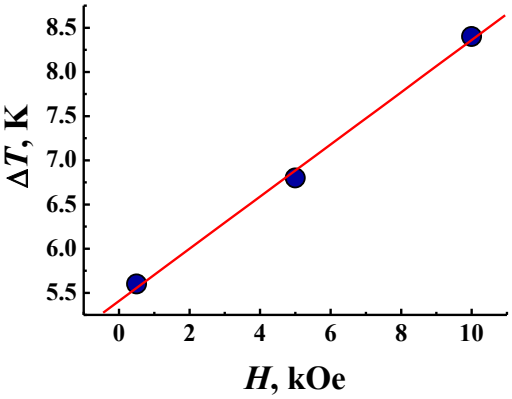


**Fig. 7.** Field dependence of the spin reorientation temperature shift ΔT(H). The solid line shows the approximation by a linear function

## 4 Conclusions

The sharp decrease of magnetization practically to zero of ordered arrays of ε-$In_{0.24}Fe_{1.76}O_3$ nanowires in the vicinity of 190 K was detected. The temperature variations of the nanowire magnetization are described by Bloch's law 3/2 taking into account the spontaneous rotation of their light magnetization axis (spin-reorientation transition). The mechanisms of nanowire remagnetization and the values of key microscopic parameters of the nanowire spin system and exchange interaction in them (spin-wave stiffness and exchange integral) have been determined. The correspondence between the exchange integrals determined within the framework of the theory of elementary magnon excitations,

the number of which grows according to the 3/2 law, and the Weiss molecular field approximation has been established.

Measurements of magnetic properties in the spin reorientation region reveal a temperature hysteresis during cooling and heating of ε-$In_{0.04}Fe_{1.96}O_3$, nanoparticles, which is typical for a phase transition of the first kind. Contributions of high-temperature phase with high value of magnetization and low-temperature phase with low value of magnetization in total magnetization of ε-$In_{0.04}Fe_{1.96}O_3$ nanoparticles were separated. The basic thermodynamic regularities of the magnetic phase transition were established. The enthalpies and entropies as well as other thermodynamic characteristics of the spin-reorientation transition registered in different magnetic fields were determined. The spin-reorientation transition was found to be magnetosensitive.

## 5 Acknowledgements

This work was carried out under Government Assignment #AAA19-119092390079-8. The authors are grateful to R.B. Morgunov for providing samples.

## References

1. L. Machala, J. Tucek, R. Zboril, Polymorphous transformations of nanometric iron (III) oxide: a review Chemistry of Materials, **23(14)**, 3255–3272 (2011) DOI: 10.1021/cm200397g
2. R. Zboril, M. Mashlan, D. Petridis, Iron (III) oxides from thermal processes synthesis, structural and magnetic properties, mössbauer spectroscopy characterization, and applications Chemistry of Materials, **14(3)**, 969–982 (2002) DOI: 10.1021/cm0111074
3. A. Namai, S. Sakurai, M. Nakajima, T. Suemoto, K. Matsumoto, M. Goto, S. Sasaki, S.-I. Ohkoshi, Synthesis of an electromagnetic wave absorber for high-speed wireless communication Journal of the American Chemical Society, **131(3)**, 1170–1173 (2009) DOI: 10.1021/ja807943v
4. A. Namai, M. Yoshikiyo, K. Yamada, S. Sakurai, T. Goto, T. Yoshida, T. Miyazaki, M. Nakajima, T. Suemoto, H. Tokoro, S. Ohkoshi, Hard magnetic ferrite with a gigantic coercivity and high frequency millimetre wave rotation Nature Communications, **3**, 1035, (2012) DOI: 10.1038/ncomms2038
5. D. Peeters, D. Barreca, G. Carraro, E. Comini, A. Gasparotto, C. Maccato, C. Sada, G. Sberveglieri, Au/ε-Fe2O3 nanocomposites as selective NO2 gas sensors Journal of Physical Chemistry C, **118(22)**, 11813–11819 (2014), DOI: 10.1021/jp5032288
6. L. Kubickova, P. Brazda, M. Veverka, O. Kaman, V. Herynek, M. Vosmanska, P. Dvorak, K. Bernasek, J. Kohout, Nanomagnets for ultra-high field MRI: magnetic properties and transverse relaxivity of silica-coated ε-Fe2O3 Journal of Magnetism and Magnetic Materials, **480(15)**, 154–163 (2019) DOI: 10.1016/j.jmmm.2019.02.067
7. J. G. Li, G. Fornasieri, A. Bleuzen, M. Gich, M. Imperor-Clerc, ε-Fe2O3 nanocrystals inside mesoporous silicas with tailored morphologies of rod, Platelet and Donut Chemistry of nanomaterials for energy, biology and more, **4(11)**, 1168–1176 (2018) DOI: 10.1002/cnma.201800266
8. A. Tanskanen, M. Karppinen, Tailoring of optoelectronic properties of ε-Fe2O3 thin films through insertion of organic interlayers Physica status solidi (RRL), **12(12)**, 1800390 (2018) DOI: 10.1002/pssr.201800390
9. K. Kralovec, R. Havelek, D. Koutova, P. Veverka, L. Kubickova, P. Brazda, J. Kohout, V. Herynek, M. Vosmanska, O. Kaman, Magnetic nanoparticles of Ga-substituted ε-

Fe2O3 for biomedical applications: magnetic properties, transverse relaxivity, and effects of silica-coated particles on cytoskeletal networks Journal of Biomedical Materials Research Part A, **108(7)**, 1563–1578 (2020) DOI: 10.1002/jbm.a.36926

10. M. Gich, C. Frontera, A. Roig, J. Fontcuberta, E. Molins, N. Bellido, C. Simon, C. Fleta, Magnetoelectric coupling in ε-Fe2O3 nanoparticles Nanotechnology, **17(3)**, 687–691 (2006) DOI: 10.1088/0957-4484/17/3/012
11. J. Tucek, R. Zboril, A. Namai, S. Ohkoshi, ε-Fe2O3: an advanced nanomaterial exhibiting giant coercive field, millimeter-wave ferromagnetic resonance, and magnetoelectric coupling Chemistry of Materials, **22(24)**, 6483–6505 (2010) DOI: 10.1021/cm101967h
12. H. Tokoro, A. Namai, S. Ohkoshi, Advances in magnetic films of epsilon-iron oxide toward next-generation high-density recording media Dalton Transactions, **50(2)**, 452–459 (2021) DOI: 10.1039/D0DT03460F
13. S. Sakurai, J. Jin, K. Hashimoto, S. Ohkoshi, Reorientation phenomenon in a magnetic phase of ε-Fe2O3 nanocrystal Journal of the Physical Society of Japan, **74(7)**, 1946–1949 (2005) DOI: 10.1143/JPSJ.74.1946
14. S. Sakurai, S. Kuroki, H. Tokoro, K. Hashimoto, S. Ohkoshi, Synthesis, crystal structure, and magnetic properties of ε-InxFe2-xO3 nanorod-shaped magnets Advanced Functional Materials, **17(14)**, 2278–2282 (2007) DOI: 10.1002/adfm.200600581
15. K. Yamada, H. Tokoro, M. Yoshikiyo, T. Yorinaga, A. Namai, S. Ohkoshi, The phase transition of ε-InxFe2-xO3 nanomagnets with a large thermal hysteresis loop Journal of Applied Physics, **111(7)**, 07B506 (2012) DOI: 10.1063/1.3672075
16. A. I. Dmitriev, H. Tokoro, S. Ohkoshi, R. B. Morgunov, Anomalous magnetization dynamics near the spin-reorientation transition temperature in ε-In0.24Fe1.76O3 nanowires Low Temperature Physics, **41(20)**, 20–24 (2015) DOI: 10.1063/1.4906312
17. M. Gich, A. Roig, C. Frontera. E. Molins, J. Sort, M. Popovici, G. Chouteau, D. Martin y Marero, J. Nogues, Large coercivity and low-temperature magnetic reorientation in ε-Fe2O3 nanoparticles Journal of Applied Physics, **98(4)**, 044307 (2005) DOI: 10.1063/1.1997297
18. A. I. Dmitriev, O. V. Koplak, A. Namai, H. Tokoro, S. Ohkoshi, R. Morgunov, Magnetic Phase Transition in ε-InxFe2–xO3 Nanowires Physics of the Solid State, **55(11)**, 2252–2259 (2013) DOI: 10.1134/S1063783413110073
19. A. I. Dmitriev, O. V. Koplak, A. Namai, H. Tokoro, S. Ohkoshi, R. B. Morgunov, Spin-reorientation transition in ε-In0.24Fe1.76O3 nanowires Physics of the Solid State, **56(9)**, 1795–1798 (2014) DOI: 10.1134/S1063783414090091
20. M. Sperl, A. Singh, U. Wurstbauer, S. Kumar Das, A. Sharma, M. Hirmer, W. Nolting, C. H. Back, W. Wegscheider, G. Bayreuther, Spin-wave excitations and low-temperature magnetization in the dilute magnetic semiconductor (Ga,Mn)As Physical Review B, **77(12)**, 125212 (2008) DOI: 10.1103/PhysRevB.77.125212
21. B. Martinez, A. Roig, X. Obradors, E. Molins, Magnetic properties of γ-Fe2O3 nanoparticles obtained by vaporization condensation in a solar furnace Journal of Applied Physics, **79(5)**, 2580–2586 (1996) DOI: 10.1063/1.361125
22. G. Xiao, C. L. Chien, Temperature dependence of spontaneous magnetization of ultrafine Fe particles in Fe-SiO2 granular solids Journal of Applied Physics, **61(8)**, 3308–3310 (1987) DOI: 10.1063/1.338891

23. V. B. Barbeta, R. F. Jardim, P. K. Kiyohara, F. B. Effenberger, L. M. Rossi, Magnetic properties of Fe3O4 nanoparticles coated with oleic and dodecanoic acids Journal of Applied Physics, **107(7)**, 073913 (2010) DOI: 10.1063/1.3311611
24. S. T. B. Goennenwein, T. Graf, T. Wassner, M. S. Brandt, M. Stutzmann, J. B. Philipp, R. Gross, M. Krieger, K. Zürn, P. Ziemann, A. Koeder, S. Frank, W. Schoch, A. Waag, Spin wave resonance in Ga1-xMnxAs Applied Physics Letters, **82(5)**, 730–732 (2003) DOI: 10.1063/1.1539550
25. K. P. Belov, A. K. Zvezdin, A. M. Kadomtseva, R. Z. Levitin, Spin-reorientation transitions in rare-earth magnets Soviet Physics Uspekhi, **19(7)**, 574–596 (1976) DOI: 10.1070/PU1976v019n07ABEH005274
26. C. P. Slichter, H. G. Drickamer, Pressure-induced electronic changes in compounds of iron, Journal of Chemical Physics, **56(5)**, 2142–2160 (1972) DOI: 10.1063/1.1677511
27. F. A. Fedulov, D. V. Saveliev, D. V. Chashin, S. B. Odinokov, A. S. Kuznetsov, Y. K. Fetisov, Anisotropy of magnetoelectric effects in a planar heterostructure comprising a piezoelectric substrate and a ferromagnetic grating, Journal of Magnetism and Magnetic Materials, **547**, 168943 (2022) https://doi.org/10.1016/j.jmmm.2021.168943